ARTICLE

BIOTECHNOLOGY and BIOENGINEERING

Recreating the Perivascular Niche Ex Vivo Using a Microfluidic Approach

Bita Carrion,[1] Carlos P. Huang,[2] Cyrus M. Ghajar,[2,3] Suraj Kachgal,[2] Ekaterina Kniazeva,[2] Noo Li Jeon,[1,2,4] Andrew J. Putnam[1,2,5]

[1]Department of Chemical Engineering and Materials Science, University of California-Irvine, Irvine, California

[2]Department of Biomedical Engineering, University of California-Irvine, Irvine, California

[3]Life Sciences Division, Department of Cancer & DNA Damage Responses, Lawrence Berkeley National Laboratory, Berkeley, California

[4]School of Mechanical and Aerospace Engineering, Seoul National University, Seoul, Republic of Korea

[5]Department of Biomedical Engineering, University of Michigan, 2154 Lurie Biomedical Engineering Building, 1101 Beal Ave, Ann Arbor, Michigan 48109; telephone: 734-615-1398; fax: 734-647-4834; e-mail: putnam@umich.edu

Received 4 March 2010; revision received 22 June 2010; accepted 19 July 2010

Published online 29 July 2010 in Wiley Online Library (wileyonlinelibrary.com). DOI 10.1002/bit.22891

ABSTRACT: Stem cell niches are composed of numerous microenvironmental features, including soluble and insoluble factors, cues from other cells, and the extracellular matrix (ECM), which collectively serve to maintain stem cell quiescence and promote their ability to support tissue homeostasis. A hallmark of many adult stem cell niches is their proximity to the vasculature in vivo, a feature common to neural stem cells, mesenchymal stem cells (MSCs) from bone marrow and adipose tissue, hematopoietic stem cells, and many tumor stem cells. In this study, we describe a novel 3D microfluidic device (MFD) as a model system in which to study the molecular regulation of perivascular stem cell niches. Endothelial cells (ECs) suspended within 3D fibrin gels patterned in the device adjacent to stromal cells (either fibroblasts or bone marrow-derived MSCs) executed a morphogenetic process akin to vasculogenesis, forming a primitive vascular plexus and maturing into a robust capillary network with hollow well-defined lumens. Both MSCs and fibroblasts formed pericytic associations with the ECs but promoted capillary morphogenesis with distinct kinetics. Biochemical assays within the niche revealed that the perivascular association of MSCs required interaction between their α6β1 integrin receptor and EC-deposited laminin. These studies demonstrate the potential of this physiologically relevant ex vivo model system to study how proximity to blood vessels may influence stem cell multipotency.

Biotechnol. Bioeng. 2010;107: 1024–1032.

© 2010 Wiley Periodicals, Inc.

KEYWORDS: stem cell niche; capillary; mesenchymal stem cell; pericyte; integrin; 3D culture

Correspondence to: Andrew J. Putnam

Contract grant sponsor: US National Institutes of Health
Contract grant number: R01 HL085339
Contract grant sponsor: California Institute for Regenerative Medicine
Contract grant number: RN1-00556
Contract grant sponsor: American Heart Association
Contract grant sponsor: Ministry of Education, Science and Technology
Contract grant number: R31-2008-000-10083-0
Contract grant sponsor: National Center for Research Resources of the National Institutes of Health
Contract grant number: PHS 5 P41-RR003155
Additional Supporting Information may be found in the online version of this article.

Introduction

Post-natal adult stem cell niches are composed of numerous components, including soluble growth factors, cell–cell interactions, cell–ECM adhesions, and physical forces, which coordinately regulate cell fate decisions with precise spatiotemporal control (Discher et al., 2009; Moore and Lemischka, 2006). However, the complexity and integration of these various elements remains poorly understood. Creation of artificial stem cell niches ex vivo may augment efforts to identify the specific cues that define stem cell niches, and thereby pave the way for the successful use of stem cells in regenerative medicine (Bordignon, 2006; Fuchs et al., 2004; Scadden, 2006). To date no suitable method has been developed to fully recapitulate stem cell microenvironments, partly due to a poor understanding of in vivo niches.

A combination of appropriate soluble factors and ECM molecules that govern stem cell niches is thought to hold the

© 2010 Wiley Periodicals, Inc.

key to ex vivo manipulation (Fuchs et al., 2004; Moore and Lemischka, 2006; Srivastava and Ivey, 2006). The physical properties of stem cell microenvironments may be equally important for determining stem cell fate (Engler et al., 2006). However, recent studies suggest another feature common to many adult stem niches may be critically important in the regulation of cell fates: their physical proximity to the vasculature. This anatomic location, the so-called perivascular niche, has been suggested as the in vivo location of adult neural stem cells (NSCs; Shen et al., 2004, 2008; Tavazoie et al., 2008), MSCs from bone marrow and multiple other adult tissues (Crisan et al., 2008), and hematopoietic stem cells (Kiel and Morrison, 2008). It has even recently been proposed that all MSCs are pericytes, and that this anatomic location may enable MSCs to mobilize for repair following injury, and thereby facilitate tissue homeostasis (Caplan, 2008). In prior studies, we have used a 3D fibrin-based cell culture model to explore the mechanisms by which mesenchymal cells (either fibroblasts or MSCs) stimulate capillary formation from human umbilical vein endothelial cells (HUVECs) (Ghajar et al., 2006, 2008). While such a system yields pericyte-invested capillaries with hollow lumens that are capable of perfusing tissues in vivo (Chen et al., 2009), the ability to simultaneously control the spatial and temporal presentation of other niche-specific cues (e.g., soluble growth factors, cell–cell interactions) limited the potential of our existing system to carefully study perivascular niches ex vivo.

To better understand the importance of the perivascular location of many adult stem cell niches, we developed a simple 3D microfluidic device (MFD) that sustains capillary morphogenesis. This versatile platform contains discrete microchannels into which cells suspended in gel precursor solutions can be injected. Multiple channels can be patterned with distinct cell populations, and even in distinct ECM gels, and then subjected to diffusible gradients of soluble morphogens. In addition to the ability to support a 3D matrix environment that closely mimics the physiological conditions in which capillary morphogenesis occurs, the optical clarity and relatively thin profile of the MFD allow for higher resolution images, while the small volumes allow valuable reagents to be conserved. HUVECs, initially segregated from stromal cells (either fibroblasts or MSCs) in discrete channels, executed a morphogenetic process akin to vasculogenesis, beginning with the formation of a primitive vascular plexus and maturing into a robust, pericyte-invested capillary network with hollow well-defined lumens. Both fibroblasts and MSCs adopted pericytic locations within this system but promoted capillary morphogenesis with distinct kinetics. Because the perivascular localization of MSCs is effectively recapitulated in this simple MFD, we then demonstrated its utility as an artificial perivascular niche, revealing the novel discovering that the interaction between HUVEC-deposited laminin and the $\alpha_6\beta_1$ integrin adhesion receptor on the MSCs is required for the proper perivascular localization of MSCs.

Materials and Methods

Cell Isolation and Culture

HUVECs, freshly harvested umbilical cords as previously described (Ghajar et al., 2006), were grown in endothelial growth medium (EGM-2; Lonza, Walkersville, MD). Primary normal human lung fibroblasts (NHLFs; Lonza) were cultured in Medium 199 (Invitrogen, Carllsbad, CA) with 10% fetal bovine serum (FBS; Media Tech, Manassas, VA), 1% penicillin/streptomycin (P/S; Media Tech), and 0.5% gentamicin (GM; Invitrogen). Human mesenchymal stem cells (MSCs; Lonza) were grown in Dulbecco's modified Eagle's medium (DMEM; Invitrogen) supplemented with 10% FBS, 1% P/S, and 0.5% GM. NHLFs and MSCs were used prior to passage 10, and HUVECs at passage 3.

Microfluidic Device Design and Fabrication

MFDs were fabricated using polydimethylsiloxane (PDMS; Sylgard 184) and soft lithography as previously described (Huang et al., 2009). The device consists of two parallel main channels that are 1.5 mm wide and 50 μm tall (Fig. 1a). These are separated by three smaller chambers that are 400 μm wide × 50 μm tall, into which gel precursor solutions can be injected (Fig. 1b). All the channels are interconnected to allow media, nutrients, and cell-secreted proteins to be transported throughout the system. The main channels provide media and nutrients to support cell culture, while the gel chambers are designed to support 3D microscale tissues. The gel chambers are separated by micropillars, or posts, which influence surface tension between the gel precursor solutions and the PDMS walls and thereby control where gel formation occurs, as previously described (Huang et al., 2009). The chambers easily accommodate gels of virtually any identity (Huang et al., 2009), but here we utilized fibrin based in part on our prior studies showing the ability of fibrin gels to sustain capillary morphogenesis in 3D (Ghajar et al., 2006, 2008).

Fabrication of 3D Cellular Gel Constructs in MFDs

To embed cells in 3D gel constructs within the MFD, cells were suspended in 100 μL prepolymer solutions containing 2.5 mg/mL bovine fibrinogen (Sigma, St. Louis, MO) and 2 μL of thrombin (50 U/mL; Sigma). From this 100 μL cell suspension, 20 μL was immediately withdrawn and pipetted into the inlet reservoirs of the gel chamber sections (Fig. 1). HUVECs (1×10^6 cells/mL) and stromal cells (NHLFs or MSCs, 5×10^6 cells/mL) were embedded separately in discrete gel channels at a constant 1:5 ratio. The cell-seeded gel constructs were allowed to polymerize for 20 min at 37°C and 5% CO_2. Following polymerization, the inlet reservoirs of the main channels were filled with 200 μL of EGM-2 medium, which was suctioned through the main flow

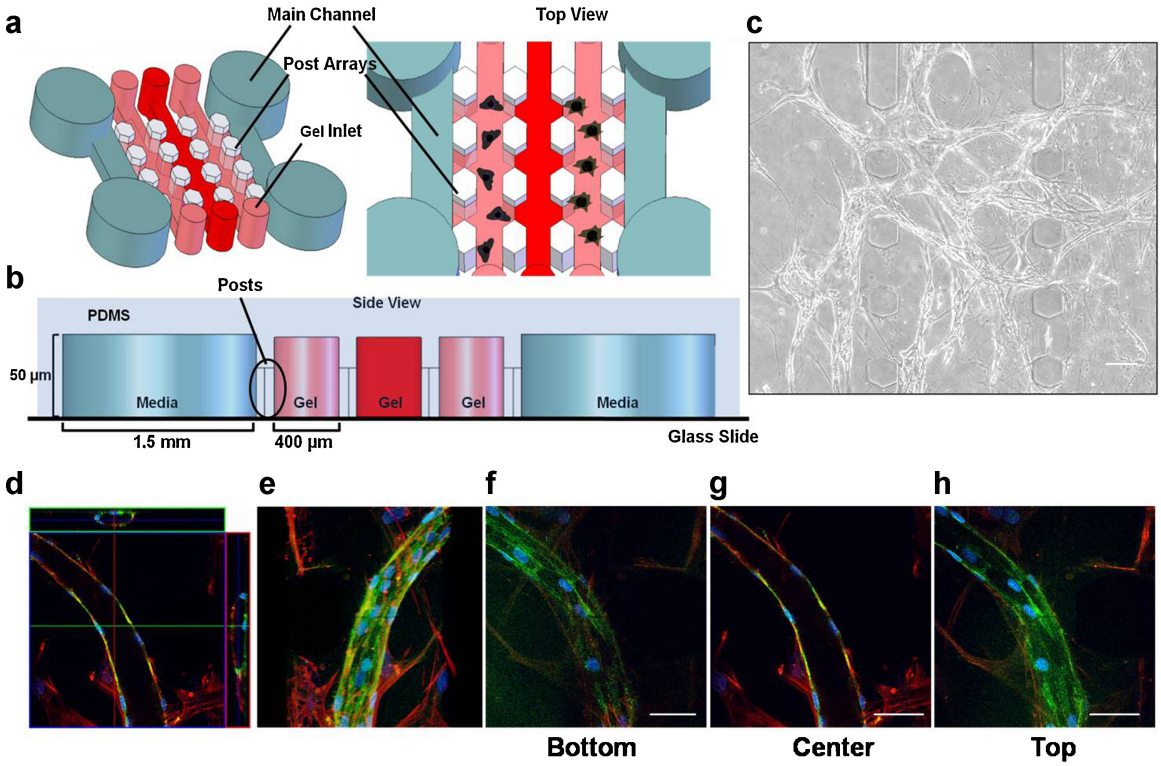

Figure 1. Formation of capillary-like networks in 3D fibrin gels within MFDs. **a**: Schematic representation of MFD showing two parallel main channels, which provide media and nutrients to the gel channels to support cell culture. Gel channels (400 μm wide each) are injected with hydrogels through the gel inlets and are separated by periodic hexagonal posts (100 μm in diameter) designed to contain hydrogels during the injection process. **b**: Side view of the PDMS device shows the location of polymerized hydrogels relative to the media channels (1.5 mm wide) and the hexagonal posts. Each microchannel is 50 μm tall. **c**: Phase-contrast image (day 14) of a primitive capillary plexus formed by HUVECs in the presence of stromal fibroblasts within fibrin gels in the MFD. Scale bar = 100 μm. **d–h**: High magnification (63×) confocal images from day 14 co-cultures stained for F-actin (with tetramethylrhodamine (TRITC)-conjugated phalloidin, red) and CD31 (with a FITC-conjugated donkey anti-mouse secondary, green). The nuclei were stained with DAPI in blue. d: Confocal images shown in an orthogonal display mode highlight the XZ and the YZ views of the image stack (top and side of image), confirming the presence of hollow lumens. e: Confocal images were stacked to obtain a 3D projection image. f–h: A series of confocal slices was taken at 800 nm intervals in the *z*-direction from the bottom, center, and top sections of the sample being imaged, respectively. The entire thickness of the section of sample being imaged is 26 μm. Scale bar = 50 μm. [Color figure can be seen in the online version of this article, available at wileyonlinelibrary.com.]

channels to wet them with media. All four inlet/outlet main channel reservoirs were then filled with EGM-2 culture medium, and the entire system incubated at 37°C and 5% CO_2 in a standard cell culture incubator. The existing medium from the main channel reservoirs was removed and replaced with fresh medium daily. Experiments were performed for up to 14 days in MFDs.

Fluorescent Labeling of HUVECs for Both Live-Cell and Fixed-Cell Imaging

In some experiments, HUVECs were fluorescently tagged using either red fluorescent protein (RFP) or cell tracker dyes in order to facilitate visualization of the capillary networks (Supplementary Movies 1 and 2). RFP labeling was achieved via retroviral transduction using the Phoenix Retrovirus Expression Kit (Orbigen, San Diego, CA) as previously described (Ghajar et al., 2008). For experiments involving the cell tracker dyes, SP-DilC_{18}(3) (D7777) and SP-DilC_{18}(3) (D7778) (Invitrogen), cells were labeled according to the manufacturer's protocol. In other experiments, cells within 3D fibrin gels in MFDs were fixed and stained for fluorescent imaging at defined end points. The various staining buffers were added and removed via the inlet/outlet reservoirs of the MFDs. The incubation times for different stages of a typical staining procedure were extended to allow for diffusion across the 3D gel constructs. Fixed and permeabilized cells within the MFDs were incubated with primary antibodies overnight at 4°C, while appropriate secondary antibodies for incubated for 3 h at 4°C. Cell nuclei were stained with DAPI, 1 mg/mL (Sigma) in PBS for 10 min. The following antibodies were used in this study: monoclonal mouse anti-human CD31, endothelial cell antibody, 1:100 (Dako, Glostrup, Denmark); monoclonal mouse α-smooth muscle actin (α-SMA), 1:200 (Abcam, Cambridge, MA); GoH3 rat monoclonal anti-α6 integrin, rat IgG (Millipore, Temecula, CA); monoclonal mouse laminin, 1:100 (Abcam); fluorescein (FITC)-conjugated donkey anti-mouse IgG secondary antibody, 1:100 (Jackson ImmunoResearch, West Grove, PA); Alexa Fluor 488 goat anti-mouse IgG secondary antibody, 1:400 (Invitrogen).

F-actin was also stained in some samples using rhodamine phalloidin, 1:250 (Invitrogen).

Confocal Imaging

Capillary networks were visualized in 3D within MFDs using a Zeiss LSM 510 Meta multiphoton microscope (Carl Zeiss, Jena, Germany). Lasers with 488 and 564 nm wavelengths were used to illuminate samples. Using a 63× oil immersion and a 40× water immersion Plan-Apochromat objectives, Z-stack images were generated by scanning every 1.2 μm through samples 20–50 μm in thickness. Individual images of a Z stack were then merged using LSM Image Browser Software (Carl Zeiss) to generate 3D projections. These methods were used to qualitatively demonstrate the presence of hollow lumens within the capillary networks, and to visualize interactions between the stromal cells and the HUVECs.

Quantitative Analysis of Capillary-Like Structures

The rate of capillary network formation within MFDs was quantified by determining the area occupied by multicellular endothelial cord-like structures at discrete time points. Cord segments comprising RFP-labeled HUVECs were imaged at multiple time points within randomly chosen sections of the gels via an Olympus IX51 microscope equipped with a 100-W high pressure mercury lamp (Olympus America, Center Valley, PA) and QImaging camera. The fluorescent images acquired using QCapture Pro Software were then processed using open-source image processing software (NIH ImageJ, National Institute of Health, Bethesda, MD) as previously described (Ghajar et al., 2007). Briefly, fluorescent images of cord segments with defined edges were sharpened and thresholded. Next, these thresholded regions were traced, and the area occupied by these thresholded regions was finally calculated and summed to yield a percentage of the total image area occupied by the cord segments (Supplementary Fig. 2). These cord-like segments were confirmed to ultimately develop into capillary networks with hollow lumens after 7 days in culture (Supplementary Movies).

Integrin-Blocking Studies in MFDs

The role of the interaction between $\alpha_6\beta_1$ integrin and laminin in the perivascular association of MSCs and capillaries was assessed using an anti-α_6 integrin monoclonal antibody (GoH3; Millipore). First, the optimal concentration of antibody required to block MSC adhesion was identified using standard cell adhesion assays as previously described (Kikkawa et al., 1994). Briefly, 96-well microtiter plates (Nunc, Wiesbaden, Germany) were coated with natural mouse laminin (10 μg/mL) at 37°C for 1 h and then blocked with PBS containing 1% BSA for another hour. Rat monoclonal antibodies against α6 integrin at three different concentrations (24, 30, and 40 μg/mL) were pre-incubated with MSC suspensions (3×10^5 cells/mL) in serum-free DMEM for 15 min; then 0.1 mL of the cell suspension was added to each well of the 96-well plate. Cells were incubated at 37°C for 1 h, at which point non-adherent cells were washed away. The attached cells were fixed and stained with a 0.4% crystal violet in methanol (w/v) for 30 min. After washing with distilled water, the stain was extracted with 0.1 M citrate in 50% ethanol. The absorbance of each well of the plates was measured at 590 nm with a microplate reader (Bio-Rad, Philadelphia, PA).

Using the results from these adhesion-blocking assays, MFDs with MSC–HUVEC co-cultures (5:1 ratio of MSCs to HUVECs) were used to explore the role of this integrin in their interaction. MSCs were cultured in serum-free DMEM for 2 days prior to seeding within the MFDs. They were then pre-incubated with anti-α6 integrin blocking antibody at 40 μg/mL concentration for 20 min prior to seeding them within 2.5 mg/mL fibrin gels in one of the side channels. HUVECs were seeded within fibrin gels in the other side channel. A middle channel containing only fibrin physically separated the two populations of cells. Experiments were performed for up to 3 days in MFDs. A complementary experiment where the anti-integrin blocking antibody was added to intact vessels was also performed to determine if pericytes would dissociate from HUVECs. In these experiments, MSC–HUVEC co-cultures (5:1 ratio) were established in MFDs for 7 days, enabling the formation of HUVEC-lined capillaries surrounded by MSCs as pericytes. Cultures were then incubated with anti-α6 integrin blocking antibody at 40 μg/mL concentration for additional 4 days.

Statistical Analysis

Statistical analysis was carried out using GraphPad Prism software. Data are reported as means ± standard deviations. All statistical comparisons were made by performing a one-way analysis of variance (ANOVA), followed by Bonferroni's multiple comparison tests to judge significance between two data sets at a time. P-values <0.05 are considered statistically significant.

RESULTS

HUVEC–Stromal Cell Co-Cultures Form Robust Capillary Networks Within MFDs

To validate the use of our MFD as a model system capable of recreating and studying the perivascular niche in 3D, one of two minimal design constraints that must be satisfied is the MFD's capacity to support vasculogenesis in a 3D gel. To satisfy this criterion, HUVECs and stromal cells were embedded separately within 2.5 mg/mL fibrin gels in two

discrete microchannels on either side of the MFDs. The microchannels were separated by an acellular microchannel in the middle, which contained only fibrin. Within 1–3 days following cell seeding, both the HUVECs and fibroblasts invaded the interstitial matrix to occupy the middle chamber. We initially used NHLFs as our population of stromal cells based on their known ability to stimulate capillary sprouting in a similar in vitro model of angiogenesis (Ghajar et al., 2008). In this vasculogenesis model, HUVECs aligned into small multicellular aggregates, or cords, and within 3–5 days appeared to form complex network structures similar to the primitive capillary plexus observed in vasculogenesis (ten Dijke and Arthur, 2007; Fig. 1c). Association between the HUVECs and fibroblasts occurred by day 7 and increased through day 14. To facilitate visualization of the capillary structures, cultures in MFDs were stained for CD31/PECAM (green), F-actin (red), and nuclei (blue). Fluorescent imaging confirmed that the HUVECs differentiated into multicellular capillary-like structures in the presence of the fibroblasts (Fig. 1d and e). The presence of hollow lumens, an important distinction of bona fide capillaries, was confirmed by confocal microscopy (Fig. 1d; see also Supplementary Movies). A series of cross-sectional images across the cord-like structures in the Z direction confirmed the presence of hollow lumens (Fig. 1f–h), a hallmark of capillary networks observed in other 3D culture systems (Ghajar et al., 2006).

MSCs Occupy a Perivascular Location Within the MFDs and Encourage HUVEC-Mediated Deposition of Basement Membrane

A second minimal design constraint that our device needed to satisfy was the capacity to support the perivascular association of MSCs with the HUVEC-derived vessel networks. We also hypothesized that the perivascular location of MSCs depends on the establishment of EC basolateral polarity and the deposition of a basement membrane, a thin network of ECM rich in laminin and collagen-IV that is a hallmark of a stable capillary network (Jain, 2003; Kalluri, 2003). Thus, it was also crucial to demonstrate the presence of a basement membrane in HUVEC–MSC co-cultures within the MFDs. To do so, capillary networks formed by co-culture of HUVECs and MSCs structures formed in the MFDs were stained for laminin at day 14, and then a series of Z-stack confocal images were captured. These images confirmed that laminin

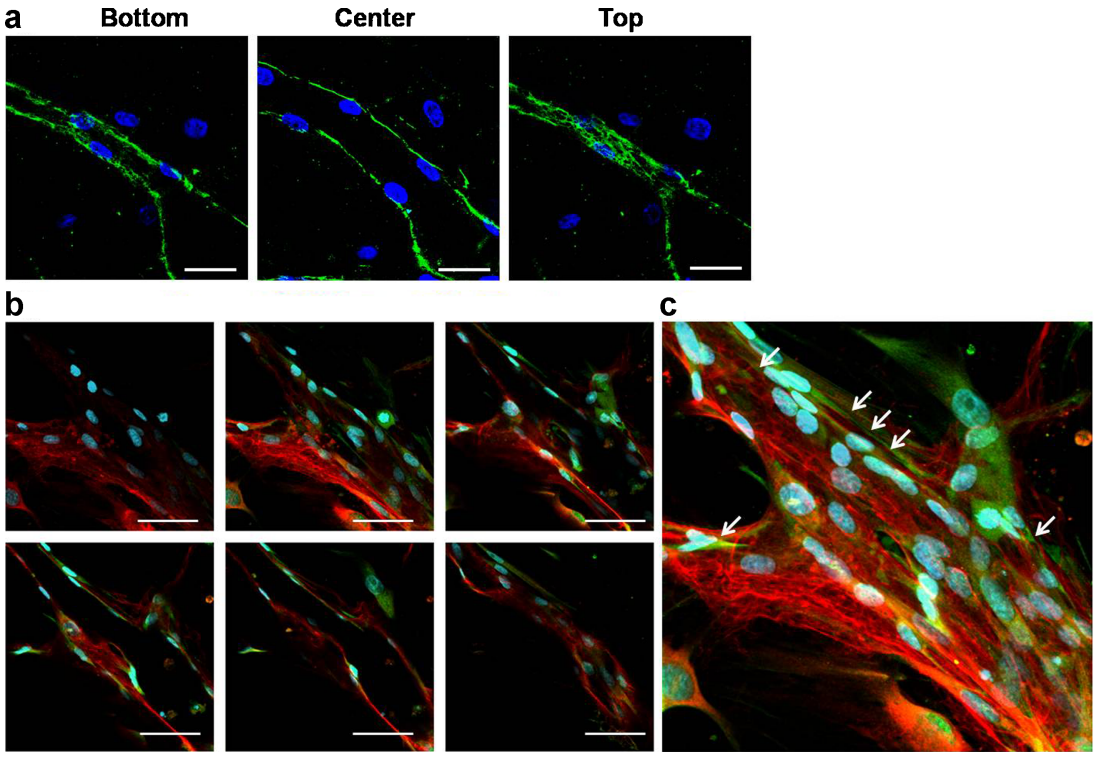

Figure 2. Basement membrane deposition and pericyte association in HUVEC–MSC co-cultures. **a**: Z-stack confocal slices demonstrate the presence of laminin (green) deposited around the basal surface of a capillary formed in a HUVEC–MSC co-culture. Scale bar = 50 μm. **b**: Confocal images from day 14 co-cultures also demonstrate an intimate perivascular association between MSCs and HUVECs in the nascent capillary network. MSCs stained for α-SMA (green) lie in close proximity to the newly deposited basement membrane (laminin, red). The top-left and bottom-right images represent the top and bottom sections of the sample, respectively. The rest of the confocal images represent a stack of four consecutive slices between the top and the bottom of the sample. Scale bar = 50 μm. **c**: High magnification (40×) confocal images were stacked to obtain the 3D projection image. In all panels, nuclei are stained with DAPI (blue). [Color figure can be seen in the online version of this article, available at wileyonlinelibrary.com.]

(green) was deposited primarily around the periphery of the vessel structures, wrapping the capillary and more clearly marking the lumens (Fig. 2a). Furthermore, MSCs were also found to act as vessel pericytes in HUVEC–MSC co-cultures within the MFDs. After 14 days of culture within the MFDs, microscale tissues were fixed and stained for α-SMA (green), a pericyte marker, and laminin (red). Confocal images showed the perivascular association of MSCs expressing α-SMA with capillary structures composed of HUVECs (Fig. 2b and c). Confocal slices taken of different XY planes at multiple depths in the Z direction confirmed that the HUVEC–MSC capillaries form hollow lumens (Fig. 2b), just as in HUVEC–fibroblast co-cultures (Fig. 1). The MSCs retained their close proximity with the nascent capillaries over time, and eventually wrapped themselves around the forming vessels.

Stromal Cells Co-Cultured With HUVECs in Fibrin Gels Differentially Affect the Kinetics of Capillary Morphogenesis Within MFDs

Having demonstrated that our MFD satisfies the two minimal design criteria to serve as an artificial perivascular niche, we next utilized it to assess if there were any differences in the rates of vessel formation induced by MSCs versus fibroblasts. Fibroblasts, MSCs, and a variety of other stromal cell types (i.e., adipose-derived stem cells) can also stimulate capillary morphogenesis, but whether or not these distinct stromal populations stimulate the ECs via the same or distinct mechanisms remains unknown. Qualitatively, fibroblasts appeared more effective than MSCs in terms of their ability to induce HUVECs to organize into multicellular cord-like network structures (Fig. 3a), despite the fact that both stromal cells eventually give rise to bona fide capillaries with hollow lumens (see Supplementary Movies). To measure these differences, we adapted a previously described image processing approach (Ghajar et al., 2007; Supplementary Fig. 2) to quantify the area occupied by RFP-expressing HUVECs in a set of randomly selected images within the MFDs. Quantitative analysis of the presence of the RFP signal within the images confirmed that the HUVEC–fibroblast co-cultures generated multicellular cord-like networks at a significantly faster rate than did the HUVEC–MSC co-cultures at both days 1 and 3 following cell seeding (Fig. 3b). Snapshots of the Supplementary Movies of day 7 cultures show that capillaries driven by fibroblasts possessed well-defined cell–cell junctions, completely enclosed lumens, and a branched morphology, whereas MSC-driven networks were less organized and less mature at the same time point (Fig. 3c and d and Supplementary Movies).

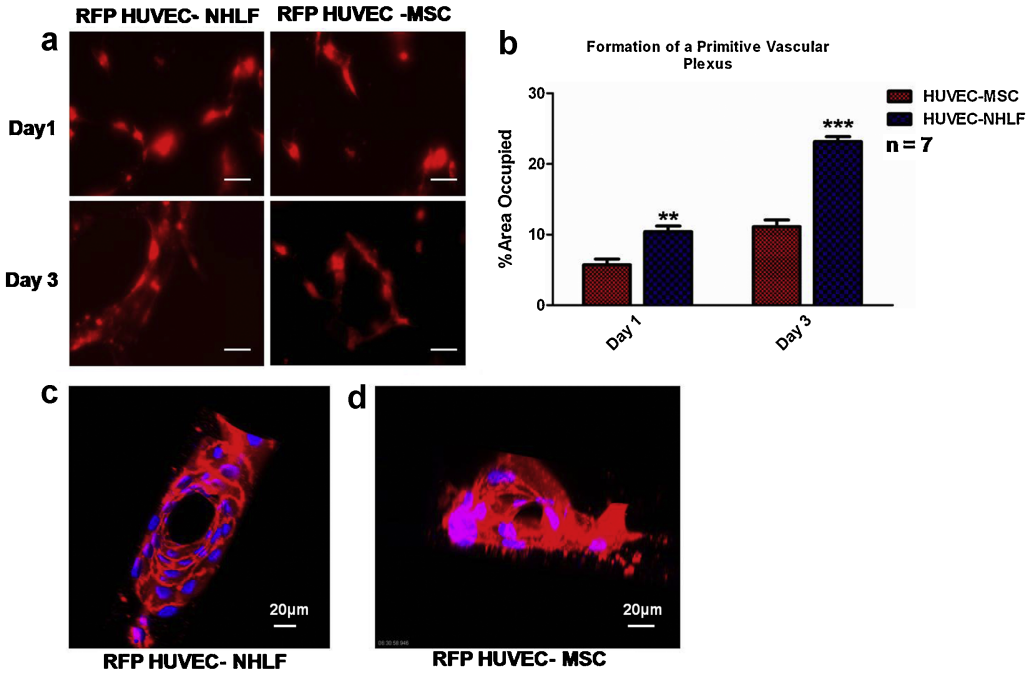

Figure 3. Differential effects of stromal cell populations on the rate of capillary morphogenesis within 3D fibrin gels in MFDs. **a**: At days 1 and 3, fluorescent images of RFP-expressing HUVECs co-cultured with either unlabeled MSCs or fibroblasts (NHLFs) were obtained from triplicate MFDs for each condition. Scale bar = 20 μm. **b**: The fluorescent areas in randomly selected images ($n = 7$) were then quantified as a metric of the extent of capillary network formation, revealing that NHLF-mediated network formation was significantly faster than MSC-mediated capillary morphogenesis ($^{***}P < 0.001$ or $^{**}P < 0.01$). **c**,**d**: Snapshots from the Supplementary Movies generated at day 7 show the presence of hollow lumens in capillary networks formed by HUVEC–NHLF co-cultures and HUVEC–MSC co-cultures. [Color figure can be seen in the online version of this article, available at wileyonlinelibrary.com.]

The Molecular Interactions Between MSCs and ECs Were Probed Using the Ex Vivo Perivascular Niche

Finally, we utilized our microfluidic ex vivo model of the perivascular niche to test the hypothesis that MSCs require an $\alpha_6\beta_1$ integrin–laminin interaction to occupy a periendothelial location. This hypothesis is based on the fact that NSCs, which also occupy perivascular locations, interact with capillaries in part through their $\alpha_6\beta_1$ integrin and EC-deposited laminin (Shen et al., 2008), and we reasoned that the common perivascular location of NSCs and MSCs in vivo may be due to similar adhesive mechanisms. To investigate this possibility, it was first confirmed that MSCs express $\alpha_6\beta_1$ integrin (Supplementary Fig. 1a) and that their adhesion to laminin can be blocked in a dose-dependent fashion in the presence of a monoclonal antibody targeting the α6 integrin subunit (Sonnenberg et al., 1987) (Supplementary Fig. 1b). Next this antibody was used to test the requirement for the $\alpha_6\beta_1$ integrin subunit for MSC–EC interactions in the MFD-based ex vivo perivascular niche. HUVEC–MSC co-cultures in 3D fibrin gels were established and matured for 7 days, with the MSCs adopting a pericyte location (Fig. 4a). On day 7, the antibody targeting the α_6 integrin subunit was added to the device via one of the media channels proximal to the initial MSC compartment, allowing it to diffuse towards the capillary network. After an additional 2 and 4 days of culture, the MSCs moved away from the vascular surface and the extent of pericyte coverage was quantitatively reduced by the presence of the antibody (Fig. 4b and c), presumably due to the competition between the antibody and the laminin-rich basement membrane for the MSC's $\alpha_6\beta_1$ integrin. When the blocking antibody was introduced earlier in the culture period, before the establishment of EC–pericyte interactions, MSCs failed to migrate through the fibrin gels and did not localize adjacent to the HUVEC networks when compared to controls (Fig. 4d and e).

Discussion

In this study, we have demonstrated that a relatively simple microfluidic platform supports the formation of a stable and mature vascular network in 3D, and effectively recapitulates the perivascular localization of MSCs ex vivo. Endothelial

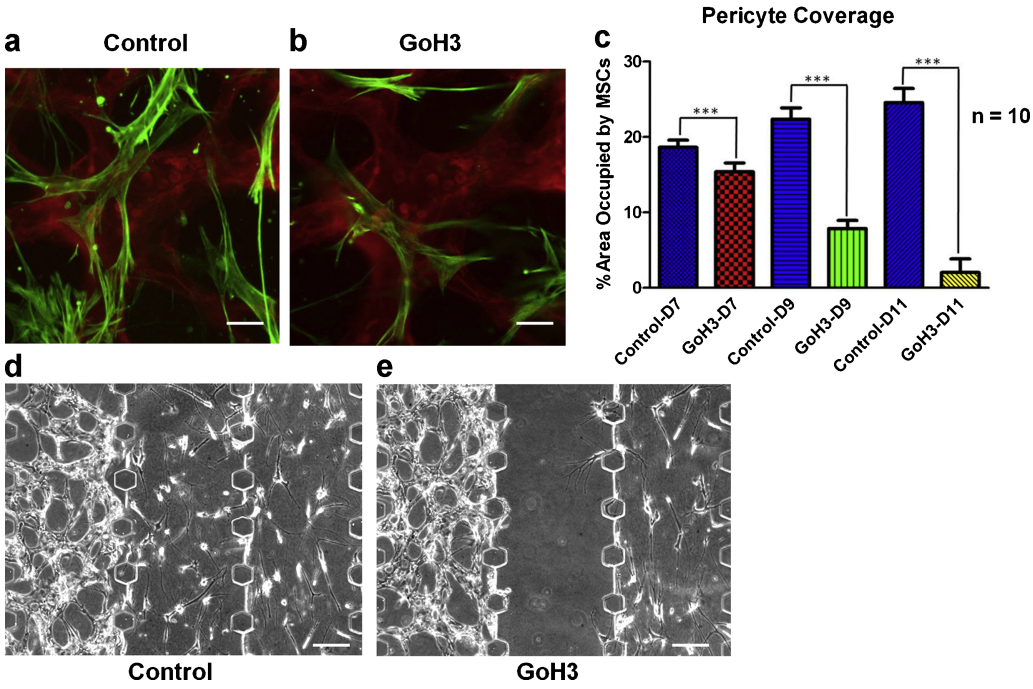

Figure 4. HUVEC–MSC interactions require the α_6 integrin subunit. **a**: Capillary networks were formed by HUVEC (red) and MSC (green) co-cultures and allowed to mature for 7 days. Cells were fluorescently labeled using cell tracker dyes. **b**: Two days after incubating the cultures containing intact capillary networks with an anti-α_6 integrin antibody, the association of MSCs with the capillary networks was disrupted. Scale bar = 50 μm. **c**: The percentage area occupied by MSCs near and around capillaries was quantified in control cultures at days 7, 9, and 11, and compared to cultures incubated with anti-α_6 integrin antibody (GoH3) for each time point. A total of 10 fluorescent images were quantified per condition (***$P < 0.001$). **d**,**e**: Phase-contrast images from day 3 HUVEC–MSC co-cultures within MFDs in the absence (control, left) or presence (right) of the anti-α_6 integrin antibody show that blocking α_6 integrin also prevents the recruitment of MSCs to the perivascular niche. Capillary networks were formed in the gels channels on the left side, and MSCs cultures were initiated on the right. Anti-α_6 integrin antibody was added to main channel on the right-hand side only, proximal to the MSCs. Scale bar = 100 μm. [Color figure can be seen in the online version of this article, available at wileyonlinelibrary.com.]

cells co-cultured with either stromal fibroblasts (NHLFs) or bone marrow-derived MSCs in this microfluidic platform undergo a vasculogenic program to yield stable, pericyte-invested capillary networks with hollow, well-defined lumens confirmed via confocal microscopy. These results recapitulate the formation of capillary structures observed in larger 3D gel cultures (Ghajar et al., 2006, 2008), demonstrating that this complex morphogenetic process can easily be scaled down to study within a MFD.

Microfluidic systems have long been touted as ideal tools with which to study multifactor regulation of cell biological phenomena, especially given their ability to deliver multiple soluble factors with precise spatial and temporal control (Mosadegh et al., 2007) and to conserve reagents based on their small size. However, the promise of such approaches has not yet been fully realized in part because most microfluidic systems involve rather cumbersome methodologies, and because their ability to support 3D cell cultures has only recently been demonstrated (Gillette et al., 2008). A promising recent study similarly utilized MFDs to develop vascular networks within 3D epithelial tissues in vitro (Sudo et al., 2009), but the quality, stability, and physiological relevance of these vessel networks lacking mature pericytes was not clear. In our study, confocal images of HUVEC–MSC and HUVEC–NHLF co-cultures seeded within 3D fibrin gels in MFDs unambiguously confirm the presence of hollow lumens (see Supplementary Movies). Moreover, both MSCs and fibroblasts occupy perivascular locations and expressed pericyte markers when cultured with HUVECs within our MFD model.

We have previously shown that both fibroblasts and MSCs are capable of supporting capillary morphogenesis in 3D fibrin gels and in vivo, and that both are capable of acting as pericytes that express α-SMA (Ghajar et al., 2010). The capillary networks formed in the presence of these two different stromal populations within our MFD also possess similar morphological characteristics. However, the vessels generated from NHLF–HUVEC co-cultures formed at a significantly faster rate than in the MSC–HUVEC co-cultures. Some distinctions in the mechanisms by which these two cell types promote capillary morphogenesis have recently been identified (Ghajar et al., 2010), and these differences may also account for the differential rates observed here as well. Although these experiments do not directly validate the utility of this platform as a tool for studying perivascular niches per se, it may be possible to utilize the small reagent volumes and amenability to high-resolution imaging offered by the MFD to identify additional mechanistic distinctions between MSCs and fibroblasts in future studies.

Many 3D culture systems already exist to study capillary morphogenesis in vitro, including those that serve as models of vasculogenesis (Chung et al., 2009) as well as those intended to model angiogenesis (Koh et al., 2008). However, the key new contribution provided by this study is the recapitulation of the perivascular niche ex vivo to mechanistically explore how MSCs interact with the vasculature. It is already widely recognized that MSCs facilitate angiogenesis in part by acting as stabilizing perictyes (Crisan et al., 2008), and that much of their potential therapeutic benefit is based on their capacity to secrete pro-regenerative (including pro-angiogenic) factors (Wagner et al., 2009). MSCs also facilitate capillary development in part by influencing the expression levels of critical matrix remodeling enzymes (Ghajar et al., 2006). However, several recent studies suggest that the perivascular location of MSCs and other adult stem cells may act as a critical anatomic cue that maintains their multilineage potential, in part due to their direct and indirect interactions with endothelial cells. NSCs, like MSCs, have also been shown to reside in perivascular niches in vivo (Shen et al., 2008; Tavazoie et al., 2008). NSCs interact with capillaries in part through the binding of their $\alpha_6\beta_1$ integrin to EC-deposited laminin, and this interaction appears to be critical for maintaining their quiescence (Shen et al., 2008). In this study, we were able to explore the interaction between MSCs and EC-deposited basement membrane in our artificial perivascular niche. We report for the first time that the α6β1 integrin receptor is required for the perivascular interactions between MSCs and capillaries, as shown by our data indicating that treating MSCs with an anti-α_6 integrin antibody prevented their perivascular association. When the antibody was added to intact vessels with perivascular MSCs, the MSCs moved away from the vascular surface in a manner similar to that observed for neural progenitor cells in mice infused with the same anti-α_6 integrin antibody in their lateral ventricle (Shen et al., 2008). Collectively, these data confirmed our hypothesis that MSCs' perivascular location requires the interaction between the laminin-rich basement membrane of the capillaries and the $\alpha_6\beta_1$ integrin adhesion receptor on MSCs for their pericytic association. Because other adult stem cells may also localize to perivascular niches in vivo via similar mechanisms, our system may facilitate efforts to dissect the consequences of this association.

Many different approaches to engineer artificial stem cell niches based on biomaterials, drug delivery, and microfluidic approaches are currently being explored (Lutolf et al., 2009). However, a common anatomic feature of many adult stem cell niches, that is, its proximity to the vasculature, may in and of itself be instructive in a way that cannot be recapitulated by the presentation of soluble and insoluble biochemical cues or by endothelial-conditioned media. Furthermore, endothelial cells may also enhance the regenerative potential of progenitor cells independent of their ability to form functional connections to the host vasculature (Kaigler et al., 2005). By leveraging the microfluidic channels within our system to present soluble biochemical cues in gradient fashion and to spatially pattern discrete biomaterials and cell types (Huang et al., 2009), the method and the supporting data presented here provide a novel way to recapitulate and study perivascular niches ex vivo, and suggest a new approach to explore the regulation of adult stem cells.

Financial support for this study was provided by the US National Institutes of Health (R01 HL085339 to A.J.P.), the California Institute for Regenerative Medicine (RN1-00556 to A.J.P.), the American Heart Association, Western States Affiliate (pre-doctoral fellowship to E.K.), and by the WCU (World Class University) program through the Korea Science and Engineering Foundation funded by the Ministry of Education, Science and Technology (R31-2008-000-10083-0 to N.L.J.). We also gratefully acknowledge confocal microscopy support from E. Gratton and M. Digman in the Laboratory for Fluorescence Dynamics at UC Irvine, a National Center for Research Resources of the National Institutes of Health (PHS 5 P41-RR003155).

References

Bordignon C. 2006. Stem-cell therapies for blood diseases. Nature 441(7097):1100–1102.

Caplan AI. 2008. All MSCs are pericytes? Cell Stem Cell 3(3):229–230.

Chen X, Aledia AS, Ghajar CM, Griffith CK, Putnam AJ, Hughes CC, George SC. 2009. Prevascularization of a fibrin-based tissue construct accelerates the formation of functional anastomosis with host vasculature. Tissue Eng Part A 15(6):1363–1371.

Chung S, Sudo R, Mack PJ, Wan CR, Vickerman V, Kamm RD. 2009. Cell migration into scaffolds under co-culture conditions in a microfluidic platform. Lab Chip 9(2):269–275.

Crisan M Casteilla L, Chen CW, Corselli M, Park TS, Andriolo G, Sun B, Zheng B, Zhang L, Norotte C, Teng PN, Traas J, Schugar R, Deasy BM, Badylak S, Buhring HJ, Giacobino JP, Lazzari L, Huard J, Peault B. 2008. A perivascular origin for mesenchymall stem cells in multiple human organs. Cell Stem Cell 3(3):301–313.

Discher DE, Mooney DJ, Zandstra PW. 2009. Growth factors, matrices, and forces combine and control stem cells. Science 324(5935):1673–1677.

Engler AJ, Sen S, Sweeney HL, Discher DE. 2006. Matrix elasticity directs stem cell lineage specification. Cell 126(4):677–689.

Fuchs E, Tumbar T, Guasch G. 2004. Socializing with the neighbors: Stem cells and their niche. Cell 116(6):769–778.

Ghajar CM, Blevins KS, Hughes CC, George SC, Putnam AJ. 2006. Mesenchymal stem cells enhance angiogenesis in mechanically viable prevascularized tissues via early matrix metalloproteinase upregulation. Tissue Eng 12(10):2875–2888.

Ghajar CM, Suresh V, Peyton SR, Raub CB, Meyskens FL, Jr., George SC, Putnam AJ. 2007. A novel three-dimensional model to quantify metastatic melanoma invasion. Mol Cancer Ther 6(2):552–561.

Ghajar CM, Chen X, Harris JW, Suresh V, Hughes CC, Jeon NL, Putnam AJ, George SC. 2008. The effect of matrix density on the regulation of 3-D capillary morphogenesis. Biophys J 94(5):1930–1941.

Ghajar CM, Kachgal S, Kniazeva E, Mori H, Costes SV, George SC, Putnam AJ. 2010. Mesenchymal cells stimulate capillary morphogenesis via distinct proteolytic mechanisms. Exp Cell Res 316(5):813–825.

Gillette BM, Jensen JA, Tang B, Yang GJ, Bazargan-Lari A, Zhong M, Sia SK. 2008. In situ collagen assembly for integrating microfabricated three-dimensional cell-seeded matrices. Nat Mater 7(8):636–640.

Huang CP, Lu J, Seon H, Lee AP, Flanagan LA, Kim HY, Putnam AJ, Jeon NL. 2009. Engineering microscale cellular niches for three-dimensional multicellular co-cultures. Lab Chip 9(12):1740–1748.

Jain RK. 2003. Molecular regulation of vessel maturation. Nat Med 9(6):685–693.

Kaigler D, Krebsbach PH, West ER, Horger K, Huang YC, Mooney DJ. 2005. Endothelial modulation of bone marrow stromal cell osteogenic potential. FASEB J 19(1):665–667.

Kalluri R. 2003. Basement membranes: Structure, assembly and role in tumour angiogenesis. Nat Rev Cancer 3(6):422–433.

Kiel MJ, Morrison SJ. 2008. Uncertainty in the niches that maintain haematopoietic stem cells. Nat Rev Immunol 8(4):290–301.

Kikkawa Y, Umeda M, Miyazaki K. 1994. Marked stimulation of cell adhesion and motility by ladsin, a laminin-like scatter factor. J Biochem 116(4):862–869.

Koh W, Stratman AN, Sacharidou A, Davis GE. 2008. In vitro three dimensional collagen matrix models of endothelial lumen formation during vasculogenesis and angiogenesis. Methods Enzymol 443:83–101.

Lutolf MP, Gilbert PM, Blau HM. 2009. Designing materials to direct stem-cell fate. Nature 462(7272):433–441.

Moore KA, Lemischka IR. 2006. Stem cells and their niches. Science 311(5769):1880–1885.

Mosadegh B, Huang C, Park JW, Shin HS, Chung BG, Hwang SK, Lee KH, Kim HJ, Brody J, Jeon NL. 2007. Generation of stable complex gradients across two-dimensional surfaces and three-dimensional gels. Langmuir 23(22):10910–10912.

Scadden DT. 2006. The stem-cell niche as an entity of action. Nature 441(7097):1075–1079.

Shen Q, Goderie SK, Jin L, Karanth N, Sun Y, Abramova N, Vincent P, Pumiglia K, Temple S. 2004. Endothelial cells stimulate self-renewal and expand neurogenesis of neural stem cells. Science 304(5675):1338–1340.

Shen Q, Wang Y, Kokovay E, Lin G, Chuang SM, Goderie SK, Roysam B, Temple S. 2008. Adult SVZ stem cells lie in a vascular niche: A quantitative analysis of niche cell–cell interactions. Cell Stem Cell 3(3):289–300.

Sonnenberg A, Janssen H, Hogervorst F, Calafat J, Hilgers J. 1987. A complex of platelet glycoproteins Ic and IIa identified by a rat monoclonal antibody. J Biol Chem 262(21):10376–10383.

Srivastava D, Ivey KN. 2006. Potential of stem-cell-based therapies for heart disease. Nature 441(7097):1097–1099.

Sudo R, Chung S, Zervantonakis IK, Vickerman V, Toshimitsu Y, Griffith LG, Kamm RD. 2009. Transport-mediated angiogenesis in 3D epithelial coculture. FASEB J 23(7):2155–2164.

Tavazoie M, Van der Veken L, Silva-Vargas V, Louissaint M, Colonna L, Zaidi B, Garcia-Verdugo JM, Doetsch F. 2008. A specialized vascular niche for adult neural stem cells. Cell Stem Cell 3(3):279–288.

ten Dijke P, Arthur HM. 2007. Extracellular control of TGFbeta signalling in vascular development and disease. Nat Rev Mol Cell Biol 8(11):857–869.

Wagner J, Kean T, Young R, Dennis JE, Caplan AI. 2009. Optimizing mesenchymal stem cell-based therapeutics. Curr Opin Biotechnol 20(5):531–536.